

## TOWARD AN ACCURATE MODEL OF METAL SORPTION IN SOILS

Randall T. Cygan, Howard L. Anderson, Sara E. Arthur, Patrick V. Brady, Carlos F. Jove-Colon, Jian-Jie Liang, Eric R. Lindgren, Malcolm D. Siegel, David M. Teter, Henry R. Westrich, and Pengchu Zhang

Sandia National Laboratories, Albuquerque, NM 87185-0750

### ABSTRACT

Radionuclide transport in soils and groundwaters is routinely evaluated in performance assessment (PA) using simplified conceptual models (*e.g.*,  $K_D$  method) to describe radionuclide sorption. However, the  $K_D$  approach with linear and reversible sorption of metal cations is rarely observed in the field. Inaccuracies of this model are typically addressed by conservativeness in the use of the chemical partitioning parameters, and often result in failed transport predictions or in increased costs for the cleanup of a site. Realistic assessments of radionuclide transport over a wide range of environmental conditions can proceed only from accurate and mechanistic models of the metal sorption process.

Our research has recently examined the sorption mechanisms and partition coefficients for  $Ba^{2+}$  (analog for  $^{226}Ra^{2+}$ ) onto soil minerals (iron oxides and clay phases) using a combination of isothermal sorption/desorption measurements, synchrotron spectroscopic analyses of metal sorbed substrates, and computer molecular modeling simulations. Research goals include 1) evaluation and quantification of the critical mechanisms and geochemical parameters that control the retardation of radionuclides on the sorbing phases in near-field soils, 2) use of atomistic computer simulations to predict radionuclide  $K_D$  values based on the partitioning of the metal cations between the solution and mineral surface, and 3) identification of the general trends in metal plume length associated with field sites. Results should improve our ability to estimate radionuclide migration at contaminated sites.

### INTRODUCTION

The sorption of metals onto mineral surfaces has significant influence on the estimates of radionuclide transport in the environment. Unfortunately, most current performance assessment (PA) tools use a simplified conceptual models for radionuclide sorption. Linear and reversible sorption (*i.e.*,  $K_D$  approach) is rarely observed in soils and groundwaters because of complex geochemical factors that can significantly affect radionuclide transport mechanisms and kinetics (*e.g.*, pH, fluid composition, ionic strength, mineral substrate structure and composition, organic complexation). Conceptual sorption model inaccuracies are typically addressed by added layers of conservativeness such as the use of low  $K_D$  values taken from default compilations of radionuclide partition coefficients. This approach often results in failed transport predictions, including such recent examples as the vadose zone transport of radioactive cesium at the DOE Hanford site and fracture flow transport of plutonium at the Nevada Test Site. Each failure decreases public confidence in the risk assessment process. Realistic assessments of

radionuclide transport and risk over a wide range of environmental conditions can proceed only from an accurate, mechanistic model of the sorption process.

The overall objective of our research is to provide a defensible, science-based understanding of radionuclide migration and retardation in contaminated environments. These results will provide better estimates of radionuclide movements in ground and surface waters, and will be applied to licensing and decommissioning of nuclear facilities and clean up of contaminated sites. We use complementary experimental and computational results to constrain sorption mechanisms and partition coefficients for radionuclide-soil pairs of relevance to Nuclear Regulatory Commission licensees at civilian nuclear facilities or decommissioned civilian nuclear facilities. We specifically rely on calculations done at the atomic level, coupled with sorption-desorption measurements that provide molecular detail, to identify and constrain the sorption process and kinetic parameters. This level of detail closes the reality gap by forcing a valid sorption model into the front end of the transport calculation. Subsequent modifications that are site-specific (*e.g.*, hydrologic fast flow paths, consideration of colloidal transport, mobilization by organic chelation, *etc.*) are then constrained to better reflect field observations, simply because they proceed from a realistic and defensible starting model.

This study attempts to assist in the development of a generalized treatment of radionuclide sorption by integrating various theoretical, experimental, and field approaches to obtain a general understanding of metal sorption in soils. Specific goals of this study include: 1) Evaluation and quantification of those critical mechanisms and geochemical parameters that control the retardation of selected divalent radionuclides on sorbing phases in near-field soils, primarily clay minerals (*e.g.*, montmorillonite) and Fe-oxides (*e.g.*, goethite-coated sands). This work involves spectroscopic characterizations of mineral surfaces by X-ray synchrotron radiation techniques for Ba<sup>2+</sup> (as an analog for Ra<sup>2+</sup>) on common soil minerals. 2) Use of atomistic computer simulations to predict radionuclide K<sub>D</sub> values based on the partitioning of the metal cations between the solution and mineral surface. Effective bulk K<sub>D</sub> values will be derived for the selected metals (Cs<sup>+</sup> and Ba<sup>2+</sup>) on each of the dominant surfaces of kaolinite clay and goethite. Calculated K<sub>D</sub> values are especially critical when they are lacking in the scientific literature or experimental data are wildly variable. Our theoretical treatment allows for strict *a priori* control of the chemical environment so that a consistent basis for evaluating the influence environmental variables on K<sub>D</sub> can be obtained. Additionally, this method may help to soundly assess the distribution of experimental K<sub>D</sub> values and potentially reduce their variance to a more meaningful and applicable level to help in the risk evaluation of a particular waste site. Finally, 3) we critically examine a number of uranium plumes from ore bodies and contaminated waste sites to identify characteristics of uranium plume movement. This approach allows a direct means of assessing plume migration that avoids the inherent uncertainty of data availability and accuracy of input parameters for reaction-transport models.

## **SORPTION OF BARIUM ON MONTMORILLONITE**

Radium, <sup>226</sup>Ra (t<sub>1/2</sub> = 1,600 years), is the decay product of uranium and thorium, either natural-occurring or discharged from uranium processing facilities (1). Compared with uranium, radium has a higher mobility in soil profile and higher accessibility to food web. The activity ratio (AR) of <sup>226</sup>Ra/<sup>238</sup>U in soil profile is about 10%, but <sup>226</sup>Ra greatly exceeds <sup>238</sup>U activity in most surface

soil (AR up to 1.8) and in vegetation (AR up to 65) (2). However, except for limited bulk study (3), the mechanisms of the interaction between radium and soil constituents such as clays, oxides and soil organic matters remain relatively unknown. To obtain a mechanistic understanding of radium interaction with soil, barium is employed here as a radium analog and is allowed to react with montmorillonite clay. Barium and radium are the alkaline earth elements, and possess similar ion radius ( $\text{Ba}^{2+} = 1.34 \text{ \AA}$  and  $\text{Ra}^{2+} = 1.43 \text{ \AA}$ ).

## Materials and Procedures

Montmorillonite (SWy-1) was obtained from the Source Clay Repository of the Clay Mineral Society (University of Missouri, Columbus, MO). Two phases of sorption experiment were conducted. In constant  $[\text{NaNO}_3]$  experiments, pH was initially adjusted to 3.5, 4.0, 5.0, 6.0, 7.0, 8.0 and 9.0 with 0.1 N  $\text{HNO}_3$  or  $\text{NaOH}$  solution. The  $[\text{NaNO}_3]$  was adjusted to 0.002 M with a 0.1 N  $\text{NaNO}_3$  solution. In the variable  $\text{NaNO}_3$  concentration experiment, sorption was measured at two pH levels: 6.2–6.5 and 7.2–7.4. Three  $\text{NaNO}_3$  concentrations, 0.002, 0.08, and 0.15 M, were used. X-ray absorption fine structure spectroscopy (XAFS) analysis was conducted using the X-11A beamline at the National Synchrotron Light Source of Brookhaven National Laboratory (NSLS/BNL). Along with the clay samples, several barium solids as well as aqueous  $\text{Ba}^{2+}$  were examined. Data were acquired at the barium  $\text{L}_{\text{III}}$ -edge of 5,274 eV. The electron beam energy was 2.5 GeV and the beam current was between 200 and 350 mA.

## Results

At a  $\text{NaNO}_3$  concentration of 0.002 M, barium sorption increased with solution pH from 0.14  $\text{mmol g}^{-1}$  at pH 4.3 to approximately 0.20  $\text{mmol g}^{-1}$  at pH 8.5. However, sorption of barium on montmorillonite is not sensitive to pH. Similar results have been previously reported (4,5). This suggests that the majority of the adsorbed cation resides on the fixed negative charge basal layer sites. Sorption via fixed charge sites is pH independent and the adsorbed barium is thought to form outer-sphere complexes on the montmorillonite surface. In contrast, the effect of  $\text{NaNO}_3$  levels on barium sorption is much more profound. In the two tested pH ranges, pH 6.2–6.5 and pH 7.2–7.4, sorption of barium is depressed from 0.18 to 0.06 and from 0.16 to 0.01  $\text{mmol g}^{-1}$ , respectively, as  $[\text{NaNO}_3]$  increases from 0.002 to 0.15  $\text{mol L}^{-1}$  (Fig. 1). The difference of the amount of adsorbed barium are from three-fold to more than one order of magnitude in the  $\text{NaNO}_3$  concentration ranging from 0.002 to 0.15  $\text{mol L}^{-1}$ . Sorption of cobalt ( $\text{Co}^{2+}$ ) and lead ( $\text{Pb}^{2+}$ ) on montmorillonite was also reported as pH insensitive and sensitive to the ionic strength, or  $\text{NaCl}$  concentration (4,5,6).

Figure 1 also provides the phase-uncorrected radial structure functions (RSF) generated from Fourier transforms over the  $k^2$ -weighted EXAFS spectra from 1.4 to 9.3  $\text{\AA}^{-1}$ . Peaks with  $R = 2.4 \text{ \AA}$  represent the Ba-O bond distance with the real distance of approximately 2.7–2.8  $\text{\AA}$ . The peaks with  $R = 3.3\text{--}3.4 \text{ \AA}$  are only observed in the Ba-montmorillonite samples and are attributed to the higher-shell coordination of adsorbed barium with Al or Si in the octahedral or tetrahedral layers of montmorillonite, respectively. There is no definitive structure determined beyond the first shell of hydrated oxygen atoms for the aqueous barium (Fig. 1). However, crystalline  $\text{Ba}(\text{OH})_2$  has a predominant peak at about 4.1  $\text{\AA}$ , as shown in Fig. 1, which corresponds a Ba-Ba

bond distance at 4.46 Å. Comparison of the reference and Ba adsorbed samples give us clear indication of surface structures.

From the observation that insensitive but measurable increase of sorption of barium at higher pH and the drastic depression of barium sorption at higher NaNO<sub>3</sub> concentration, we suggest the formation of a stronger surface complex at the montmorillonite surface in addition to sorption of barium at the base layer due to electrostatic attraction. From the EXAFS data, it is reasonable to attribute the formation of a stronger Ba-montmorillonite complex to the reaction between barium and the deprotonated hydroxyl surface group through sharing an oxygen atom with Al octahedra locating at the montmorillonite broken edge. The data presented here indicate that barium can form both inner- and outer-sphere complexes on the montmorillonite surface, instead of just the outer-sphere complex formation as previous studies have suggested.

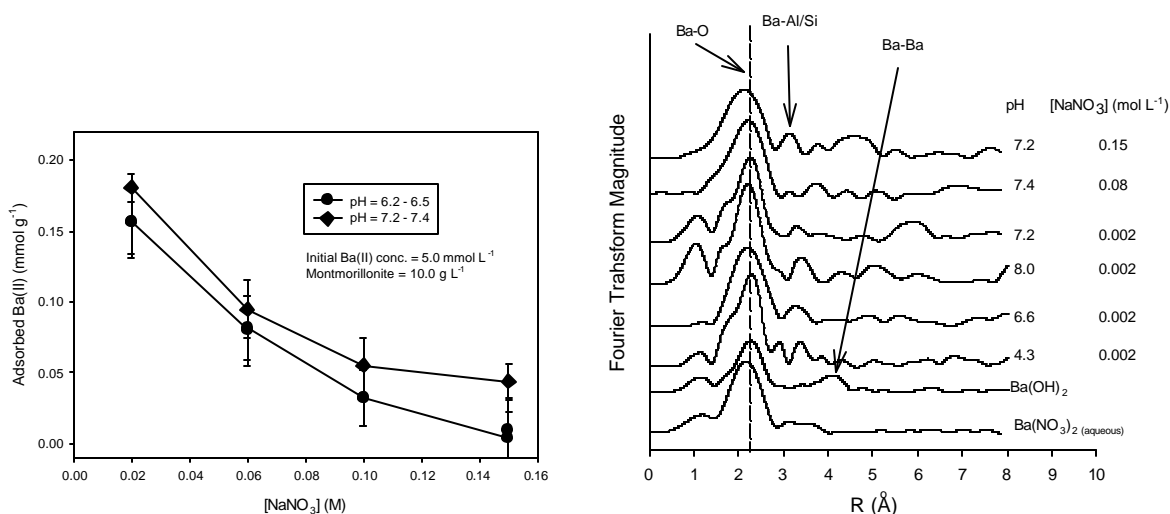


Fig 1. Effect of NaNO<sub>3</sub> concentration on barium sorption on montmorillonite at constant pH values (left) and Fourier transforms (RSF) of barium on montmorillonite surfaces under various conditions (right); Ba-Al bonding is found in all Ba-Montmorillonite spectra while Ba-Ba bond is found in only the Ba(OH)<sub>2</sub> solids; phase shift is not corrected.

## MOLECULAR DYNAMICS SIMULATION OF BARIUM SORPTION ON GOETHITE

Goethite has been identified as a surface coating phase of soil minerals common to most radioactive nuclide-contaminated sites. Even in bulk, the goethite phase exhibits high specific surface areas in excess of 200 m<sup>2</sup>/g (7). Therefore, sorption on the goethite surface will be significant, and it is critical to understand the mechanism of sorption, and subsequently the fate of common radioactive nuclides such as Cs<sup>+</sup>, Sr<sup>2+</sup>, and Ra<sup>2+</sup>, in media involving goethite phases. As part of the integrated effort of this project, we looked at the sorption of Ba<sup>2+</sup>, as an analog of radioactive Ra<sup>2+</sup>, on goethite surfaces using molecular dynamics (MD) simulation. We have paid particular attention to the various common surfaces that have been observed in natural soil goethite.

There has been a successful attempt in applying MD methods to study the clay minerals (8). Goethite bears a lot of similarities to a clay phase, such as fine grain size, occurrence of hydroxyl groups, and extensive hydrogen bonding. There had also been a direct attempt (9) using molecular mechanics to examine the goethite–water interface. These studies set the stage for a direct observation of sorption behavior of metal ions in aqueous media interfacing with the goethite phase. We have successfully examined this process by first developing a set of interatomic parameters that are suitable for large scale MD simulation of complex systems such as the goethite–Ba<sup>2+</sup> aqueous solution system. We then studied the sorption behavior by examining each individual goethite crystal surface in contact with the solution. We were able to extract local structure information such as bonding environments of the Ba<sup>2+</sup> ions, and dynamic information such as diffusion of the Ba<sup>2+</sup> ions in the system. We expect these results to help quantify the expected amount of sorption for bulk goethite by assessing the significant contributing crystal surfaces. Eventually this theoretical work may be extended to provide a theoretical estimation of the partitioning coefficient based on the energetics of sorption.

### **Molecular Dynamics Procedure**

All MD simulations were performed using the Cerius<sup>2</sup> software package and the OFF energy program (Molecular Simulations Inc.). Periodic boundary conditions were applied to eliminate edge effects. The total energy of the simulation cell was minimized, using the forcefield model and parameterization developed in the present work. A molecular dynamics simulation using constant volume and temperature (NVT) canonical ensemble was then performed at 300 K. A thermal bath was used to maintain the temperature of the simulation cell using the Hoover scheme. The Newtonian equations of motion were integrated for every one femtosecond time step. Figure 2 provides a view of the simulation cell used in the MD simulations as performed on the dominant (110) goethite surface.

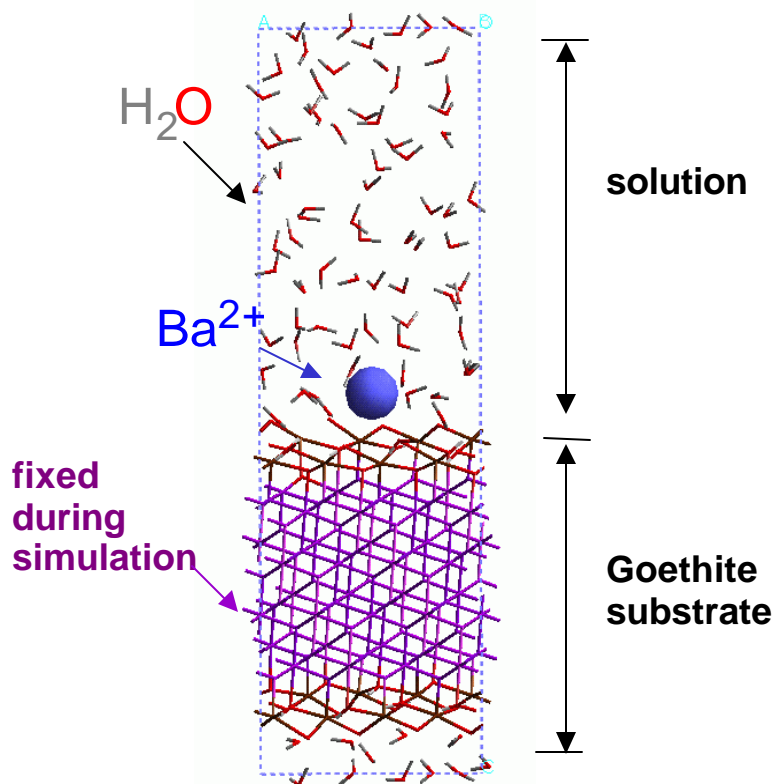


Fig. 2. Simulation cell exhibiting goethite substrate and equilibrated barium on (110) surface.

### Local Geometry of Barium Complex

Analysis of the molecular dynamics simulations provides the following details on the local geometry of the barium ion as sorbed on the various goethite surfaces. Coordination number and mean Ba-O distances of the first coordination sphere (within 4.0 Å) of Ba<sup>2+</sup> ion are given in Table I. When the Ba<sup>2+</sup> ion is in the central part of the solution portion of the simulation cell, the local structure of Ba<sup>2+</sup> is in overall agreement with that of Ba<sup>2+</sup> in bulk water (mean Ba-O distance of 2.8 Å and mean coordination number ~9). It is not known why the Ba<sup>2+</sup> coordination number (CN = 8.2) associated with the (110) surface in bulk-like environment is slightly lower. In fact, when simulating Ba<sup>2+</sup> on the (110) surface the Ba<sup>2+</sup> ion coordination number (CN = 8.5) is also lower than those of the other surfaces (CN = 9.5-9.8). There is some evidence to suggest that this lower coordination is associated with the greater ability to enhance self-diffusion of Ba<sup>2+</sup> ions on the goethite surface. When Ba<sup>2+</sup> is on the goethite surface, a general increase, relative to all goethite surfaces, of both Ba-O distance (to 2.9-3.0 Å) and Ba<sup>2+</sup> coordination number (CN = 9.5-9.8 for most surfaces) occurs. Oxygen atoms from the substrate comprise substantial portion of the coordinating environments. In the extreme case for the (101) surface, which is also the case where strongest sorption was observed, three (31%) out of 9.7 coordinating oxygens are oxygens from the substrate. Again, the percentage of the substrate oxygens in the coordinating environment is qualitatively proportional to the strength of sorption of a given surface.

Table I. Local structure of Ba<sup>2+</sup> (Ba<sup>2+</sup>-O distance and coordination number) in the goethite-water system with respect to different goethite surfaces. Numbers in brackets represent number of oxygen atoms from the substrate coordinating to the Ba<sup>2+</sup> ion.

	(110)	(020)	(101)	(021)
<b>&lt;Ba-O&gt; (Å)</b>				
<i>Bulk</i>	2.83	2.82	2.83	2.82
<i>Surface</i>	2.87	2.89	2.87	2.96
<b>CN</b>				
<i>Bulk</i>	8.2	8.8	8.9	8.7
<i>Surface</i>	8.5 [1.5]	9.5 [1.3]	9.7 [3.0]	9.8 [2.0]

Details of coordinating environment of Ba<sup>2+</sup> on goethite surfaces vary considerably from surface to surface. On the (101) surface, significant proportions of both bridging and hydroxyl oxygens are present in the first coordination sphere. On the (020) surface, only hydroxyl oxygens from the substrate are present in the first coordination sphere. The sorption on the (021) surface is not that clear-cut. While bridging oxygens dominate coordination from the substrate oxygens, hydroxyl oxygens contribute to the coordination, although in relatively small number, from the first coordination sphere continuously in terms of Ba-O distance all the way into the second coordination sphere. The (110) surface is again unique. While it is proper to use the cutoff distance of 4.0 Å for the first coordination sphere of Ba<sup>2+</sup> ion on the (101), (020), and (021) surfaces, it is not quite correct to use the same cutoff distance for Ba<sup>2+</sup> on the (110) surface. Sorption of Ba<sup>2+</sup> on the (110) surface encourages tighter (Van der Waals) bonding environment. The Ba<sup>2+</sup>-O<sub>bridging</sub> distance in the first coordination sphere is shorter than the Ba<sup>2+</sup>-O<sub>water</sub> in the same coordination sphere. On the other hand, the Ba<sup>2+</sup>-O<sub>H</sub> distance is about the same ((020) surface) or longer ((101) and (021) surface) than the Ba<sup>2+</sup>-O<sub>water</sub> distance. Therefore, surface sites containing O<sub>bridging</sub> offer stronger sorption of Ba<sup>2+</sup> than sites that contains only O<sub>H</sub> species.

The following conclusions can be made from the results of the molecular simulations: 1) a simple and reliable forcefield was developed for the dynamics simulation of goethite-water interface and sorption of radionuclide ions at these interfaces; 2) self-diffusion coefficient of Ba<sup>2+</sup> ions in water ~20 Å away from water-substrate interface (bulk water-like environment) is in the same order of magnitude (10<sup>-4</sup> cm<sup>2</sup>/s) as that of water molecules; 3) two order of magnitude differences in self-diffusion coefficients of Ba<sup>2+</sup> ions exists with regard to different surfaces of the substrate material of goethite when Ba<sup>2+</sup> ions are sorbed onto the surfaces; 4) compared to the bulk-water environment, goethite surfaces tend to induce larger coordination number and longer Ba-O distances of the first coordination sphere of the Ba<sup>2+</sup> ions; 5) it appears that surface ruggedness at atomic level is inversely proportional to the surface mobility of Ba<sup>2+</sup> ions sorbed on the surface; and 6) bridging oxygens on the exposed goethite surfaces tend to provide stronger (compared to the exposed hydroxyl oxygens) sorption sites for the Ba<sup>2+</sup> sorption.

## PREDICTION OF DISTRIBUTION COEFFICIENTS USING MOLECULAR MODELS

Molecular modeling allows us to build an atomic-level understanding of how ionic species complex with aqueous solutions and the processes by which these complexes can sorb onto mineral surfaces. These simulations can be used to develop models of sorption processes that can be compared with experimental results and used to test surface complexation models. Furthermore, we can apply these methods to develop models to predict distribution coefficients ( $K_D$ ) that describe an ionic species affinity to be sorbed to a mineral surface.

The prediction of distribution coefficients involves several critical steps: 1) the development of accurate and transferable forcefields; 2) the construction of a physically reasonable model surface and fluid; 3) the creation of molecular dynamics models that allow the surface and fluid to interact and reach an equilibrium state; and 4) defining a method for sampling the system in that allows one to define sorption and then calculate a  $K_D$  based upon the amount of ionic species sorbed relative to those species remaining in bulk solution.

We have performed simulations to test the ability of molecular-based models to predict radionuclide distribution coefficients. We previously reported the concept of the molecular dynamics approach to obtain  $K_D$  values for cesium sorption onto kaolinite (10). These preliminary simulations demonstrated the ability of a small-scale system of several thousand atoms to represent the interaction of a CsCl aqueous solution with the basal surface of kaolinite. One example indicated the sorption of approximately 63% of cesium from solution as either an inner or outer sphere sorption complex. Although the concentration values are quite high in the simulations, a distribution coefficient of approximately 12 was obtained when the results were extrapolated to a CsCl concentration of 0.001 M CsCl. This value is in general agreement with the experimental  $K_D$  of 12.

Figure 3 exhibits the simulation cell used in these latest molecular dynamics simulations. Here, the simulation cell has been expanded to include approximately 10,000 atoms. Although these cells can provide a more accurate representation of dilute solution concentrations, there is a major drawback in obtaining statistically consistent results and equilibration. Molecular simulation results for CsCl solutions (1.0 M, 0.1 M, and 0.01 M) in contact with a (001) kaolinite basal surface show that cesium is weakly sorbed as an outer sphere complex. Because of the weak bonding of this complex, the amount of cesium sorbed varies over time. Snapshots derived from molecular dynamics simulations for these surfaces over long periods of time have yet to provide the consistent statistics needed to allow the determination of a stable  $K_D$ . Simulations show that cesium is much more strongly bound to model (010) aluminol edge sites. However, the determination of a stable  $K_D$  remains elusive due to model dependence of edge site density. Simulations are in progress to evaluate the relative binding of  $Ba^{2+}$ ,  $Sr^{2+}$ , and  $Cs^+$  on kaolinite surfaces. The calculation of stable partition coefficients is difficult due to the strong dependency of the results on the model surface, the initial configuration, and the time dependent nature of weakly sorbing complexes. Additional studies will allow us to better understand the model dependence and to develop better models and statistical sampling methods. Initial results indicate that these models are able to provide a good qualitative indication for selectivity of binding at the surface and at defect sites. We are running significantly larger models (~1,000,000 atoms) for long time scales on the CPlant massively parallel computer system at



Sandia National Laboratories using the LAMMPS simulation code (11). The statistics from these larger systems will allow us to determine meaningful distribution coefficients for these model surfaces.

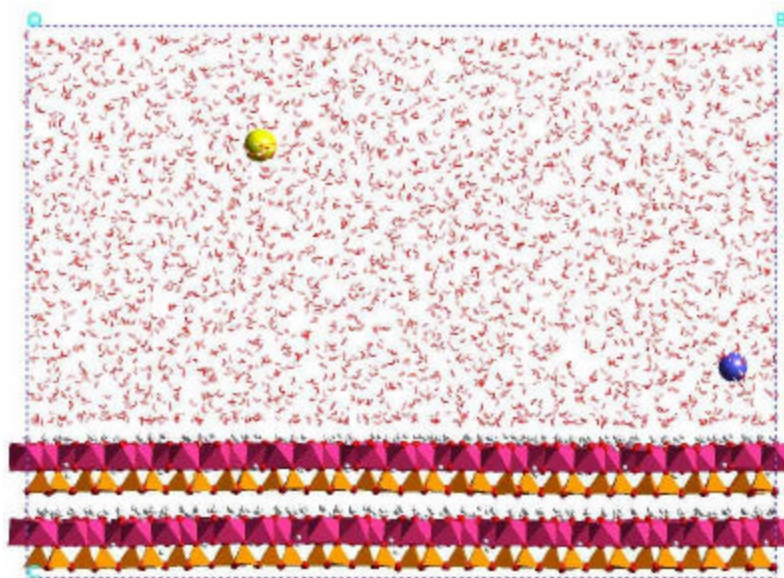


Fig. 3. Large-scale simulation cell used for the determination of distribution coefficients of cesium between aqueous phase and kaolinite surface. Cesium is represented by the dark sphere sorbed as an outer-sphere complex on the (001) basal hydroxyl surface.

## HISTORICAL CASE ANALYSIS OF URANIUM PLUME ATTENUATION

Uranium mining and processing (*e.g.*, Uranium Mill Tailing Remedial Action or UMTRA sites), and weapons testing have produced subsurface uranium plumes in groundwater. Due to concerns about remobilization of uranium to adjacent groundwater supplies, the majority of these sites are being actively remediated, while others are currently being considered for remediation. Most of these sites will need long-term monitoring for remediation and performance assessment. Natural processes, like sorption, mineral precipitation and solute dispersion occur in the absence of (and sometimes in parallel with) active remediation and together set the boundaries on how far a particular plume can move. To accurately estimate the effectiveness of remediation and to conduct long-term monitoring, it would be very useful to know the extent of these limits.

A groundwater plume of dissolved uranium originating from a point source can be expected to contain the highest dissolved contaminant levels close to the source, and gradually inferior levels down-gradient. Theoretically, the direction of maximum advance for the contaminants should be parallel to the hydrologic gradient. If the source term is removed, or somehow treated to arrest further addition of contaminant to the groundwater (*e.g.*, a landfill cap or a barrier), dilution by fresh water recharge should provoke a decrease in the levels of dissolved phase concentrations. Certainly, dilution occurring along the leading edge of a plume should eventually stop following advancement of the plume. Note that in the lack of chemical mechanisms (natural or engineered) for removal, the mass of contaminant in a plume remains unaffected by dilution. Natural mechanisms responsible for reducing the bioavailable mass of uranium in soil solutions include

reversible and/or irreversible sorption and chemical transformation, that is, the reduction of pollutant to less soluble forms. This natural reduction in mobile uranium mass likely has a tendency to accelerate the stopping of plume advance. Generally, if chemical processes are collectively the main control over plume mobility, one would expect to observe a comparable behavior in all uranium plumes. For example, we may expect all uranium plumes to attain a similar length before stopping. Knowledge of a common uranium plume cessation length would be helpful in terms of public health since it would be a primary step in evaluating the potential effect of particular plumes on groundwater. This would also allow a better assessment for allocating monitoring wells for groundwater protection. We suggest that the natural history of uranium plumes is best approached by evaluating large numbers of individual plumes following a stochastic analysis of various waste sites (12) and resolving their intrinsic characteristics of their collective advance and/or decay into specific chemical and physical processes.

Reaction-transport models entailing the prediction of contaminant transport and plume advance require extensive data inputs that often contain large uncertainties. The majority of site-specific inputs are physical parameters that can be highly variable both spatially and with time. Moreover, strong limitations in data availability and accuracy suggest that predictions based on reaction-transport models can hardly provide more than an order-of-magnitude bounding estimates of subsurface contaminant movement. A more direct way for establishing the restrictions of contaminant transport is to evaluate actual plumes to determine if, altogether, they spread and attenuate in a reasonably consistent and characteristic manner. This study entails a comprehensive characterization and comparison of uranium plumes from ore bodies and contaminated sites to identify the principal features of uranium plume movement. The scale of the original contaminant source, the geologic location, and the hydrologic regime were infrequently similar from site to site. The age of groundwater plumes varied widely and no complete collection of time-series plume analyses based on the spatial extent of uranium contamination exist for a particular site. In spite of these uncertainties and variabilities, the plume data set provided a reasonably consistent depiction of uranium plume behavior. Particularly, uranium plumes: 1) seem to attain a steady-state, that is, they stop spreading rapidly within a few years; 2) extend roughly beyond 2 km in length only in particular cases (*e.g.*, *in situ* leaching); most of the plumes are much smaller; and 3) have very similar uranium chemistry between sites. This suggests similar contaminant attenuation mechanisms regardless of their location.

### **Plume Analysis and Discussion**

The criterion used to evaluate plume behavior is the maximum surface coverage of both artificial and natural plumes or *maximum plume axial length*. However, the concept of maximum plume axial length is unavoidably operational because of the limited, random, and subjectively biased well sampling and/or monitoring performed by different workers at different sites. Furthermore, the highly distorted subsurface morphology of groundwater plumes, the occurrence of daughter plumes, and the presence of background levels of uranium adds more uncertainty as to the true extent of the 2-D surface coverage of these plumes. In order to make an objective basis of comparison, visual inspection of uranium plume contour maps and uranium concentration data in sample wells were used together to ascertain the maximum plume axial lengths. The maximum plume axial length is defined here as *the maximum distance between two points encompassing*

the farthest boundaries of the plume as constrained and/or permitted by the sampling well network in a particular site where measurable uranium concentrations in the range of 10-20 ppb have been obtained. In contrast, previous workers (13), have take into account the longest distance between the source (or highest contaminant concentration) and the plume boundary. This approach proves to be useful in intuitively evaluating the limits for possible spreading of a plume within a site if the data set is adequately large and reliable. However, for most uranium plumes, temporal and spatial limitations in well sampling, and the generation of daughter plumes through ongoing remediation activities make recognition of the source within a site a problematical duty. Considering the very limited amount of useful data, the variable spatial distribution of monitoring wells, and the scarce number of these at each site, we found that the maximum axial length offers a reasonably good estimate of the 2-D contaminant surface coverage.

Most UMTRA sites are situated within 2 or 3 km of rivers. In few cases, groundwater plumes were curtailed by discharging into rivers as expected in cases where rivers are nourished by groundwater. However, in arid regions, rivers frequently lose water to neighboring aquifers and numerous plumes extend parallel to, and sometimes away from, adjacent rivers suggesting that estimated plume lengths indicate groundwater transport. Figure 4 shows the frequency distribution of studied maximum axial plume lengths for all sites. This figure suggests that the maximum observed distance of movement is a slightly more than 2 kilometers. Abnormally long plumes (greater than 3 km) are closely associated with pervasive *in situ* leaching (ISL) such as the Konigstein mine in Germany (14,15). These are very good examples of how a plume can be readily disturbed because of manmade intervention or unnatural processes. Conversely, it seems that natural processes such as sorption, dilution, and mineral precipitation are sufficiently effective sinks to halt the short-term (years to decades) advance of artificial uranium plumes. In the case of long-term situations (*i.e.*, thousands to millions of years) like uranium mines, natural weathering processes and secondary formation of oxidized uranyl phases seems to bound quite effectively the advance of natural plumes.

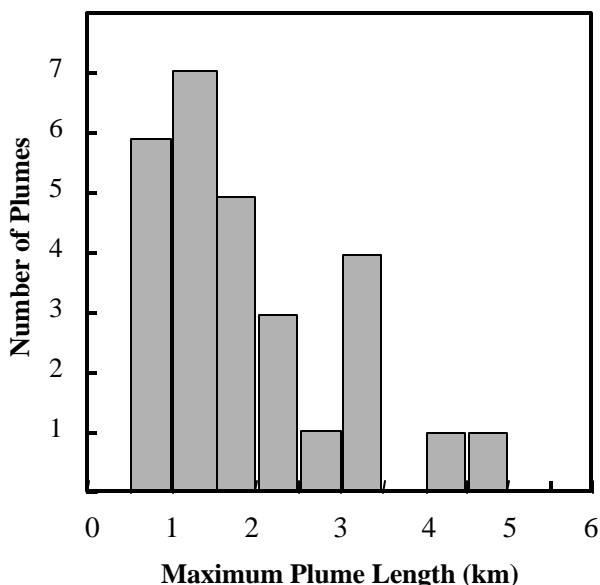


Fig. 4. Histogram of maximum plume lengths for all considered uranium plumes in this study (N=28).

## CONCLUSIONS

This research project integrates various geochemical methods to help understand the underlying mechanisms of metal sorption onto soil minerals. The combination of theoretical, experimental, spectroscopic, and field observations suggests that metal retention on mineral surfaces is variable and strongly controlled by mineral surface structure, surface chemistry, and charge distribution. The sorption of barium, as an analog to radium, occurs on both basal (outer sphere complex) and edge sites (inner sphere complex) of montmorillonite clay. Molecular dynamics simulations of barium sorption onto various surfaces of goethite indicate a variety of binding strengths and coordination environments. Forming an inner sphere complex, barium sorption onto goethite is controlled by surface hydroxyls and bridging oxygens. The binding energy is directly proportional to the number of coordinating substrate oxygens. A theoretical model can also be used to derive  $K_D$  values for selected mineral-solution systems. Active research involves the use of large-scale molecular dynamics simulations of cesium-kaolinite systems to predict distribution coefficients for metal sorption onto mineral surfaces. Finally, a historical case analysis of uranium plume lengths associated with 28 UMTRA sites suggests the attainment of a steady-state distribution of uranium within a few years. Plume lengths are approximately two kilometers in length and only exceed this value in special cases (*e.g.*, where *in situ* leaching has been carried out). The majority are much smaller. The contaminated sites exhibit very similar uranium chemistry that implies analogous mechanisms for contaminant attenuation regardless of their location.

## ACKNOWLEDGEMENTS

This research was supported by the United States Nuclear Regulatory Commission and the U.S. Department of Energy. Sandia is a multiprogram laboratory operated by Sandia Corporation, a Lockheed Martin Company, for the United States Department of Energy.

## REFERENCES

1. R. S. WANG, A. S. Y. CHAU, F. LIU, H. CHENG, P. NAR, X. M. CHEN, and Q. Y. WU, "Studies on the Adsorption and Migration of Radium in Natural Minerals," *Journal of Radioanalytical and Nuclear Chemistry*, 171, 347-364. (1993)
2. D. J. GREEMAN; A. W. ROSE, J. W. WASHINGTON, R. R. DOBOS, and E. J. CIOLKOSZ, "Geochemistry of Radium in Soils of the Eastern United States," *Applied Geochemistry*, 14, 365-385 (1999)
3. J. S. NATHWANI and C. R. PHILLIPS, "Adsorption of Ra-226 by Soils: 1.," *Chemosphere*, 5, 285-291 (1979)
4. C. C. CHEN and K. F. HAYES, "X-ray Absorption Spectroscopy Investigation of Aqueous Co(II) and Sr(II) Sorption at Clay-Water Interfaces," *Geochimica et Cosmochimica Acta*, 63, 3205-3215 (1999)
5. C. PAPELIS and K. F. HAYES, "Distinguishing Between Interlayer and External Sorption Sites of Clay Minerals Using X-ray Absorption Spectroscopy," *Colloids and Surfaces A*, 107, 89-96 (1996)

6. D. G. STRAWN, A. M. SCHEIDEGGER, and D. L. SPARKS, "Kinetics and Mechanisms of Pb(II) Sorption and Desorption at the Aluminum Oxide Water Interface," *Environmental Science & Technology*, 32, 2596-2601 (1998)
7. U. SCHWERTMANN and R. M. CORNELL, "Iron Oxides in the Laboratory," VCH, Weinheim (1991)
8. B. J. TEPPEN, K. RASMUSSEN, P. M. BERTSCH, D. M. MILLER, and L. SCHÄFER, "Molecular Dynamics Modeling of Clay Minerals: 1. Gibbsite, Kaolinite, Pyrophyllite, and Beidellite," *Journal of Physical Chemistry B*, 101, 1579-1587 (1997)
9. J. R. RUSTAD, A. R. FELMY, and B. P. HAY, "Molecular Statics Calculations for Iron Oxide and Oxyhydroxide Minerals: Toward a Flexible Model of the Reactive Mineral-Water Interface," *Geochimica et Cosmochimica Acta*, 60, 1553-1562 (1996)
10. H. R. WESTRICH, H. L. ANDERSON, S. E. ARTHUR, P. V. BRADY, R. T. CYGAN, J.-J. LIANG, P. ZHANG, and N. YEE, "Prediction of Metal Sorption in Soils," *Proceedings of the Waste Management Conference* (2000)
11. S. PLIMPTON, and B. HENDRICKSON, "A New Parallel Method for Molecular Dynamics Simulation of Macromolecular Systems," *Journal of Computational Chemistry*, 17, 326-337 (1996)
12. D. W. RICE, B. P. DOOHER, S. J. CULLEN, L. G. EVERETT, W. E. KASTENBERG, R. D. GROSE, and M. A. MARINO, "Recommendations to Improve the Cleanup Process for California's Leaking Underground Fuel Tanks," UCRL-AR-121762, Lawrence Livermore National Laboratory (1995)
13. W. W. McNAB, D. W. RICE, C. OLDENBURG, J. BEAR, C. TUCKFIELD, and R. RAGAINI, "Historical Case Analysis of CVOC Plumes," UCRL-AR-133361, Lawrence Livermore National Laboratory (1999)
14. D. BIEHLER and W. E. FALCK, "Simulation of the Effects of Geochemical Reactions on Groundwater Quality during Planned Flooding of the Konigstein Uranium Mine, Saxony, Germany," *Hydrogeology Journal*, 7, 284-293 (1999)
15. O. NITZSCHE and B. MERKEL, "Reactive Transport Modeling of Uranium 238 and Radium 226 in Groundwater of the Konigstein Uranium Mine, Germany," *Hydrogeology Journal*, 7, 423-430 (1999)